Published in final edited form as:
Curr Opin Chem Biol. 2012 April ; 16(1-2): 11–18. doi:10.1016/j.cbpa.2012.03.003.

Oxomanganese complexes for natural and artificial photosynthesis

Ivan Rivalta, **Gary W. Brudvig**, and **Victor S. Batista**
Department of Chemistry, Yale University, New Haven, Connecticut, 06520-8107, U.S.A

Abstract

The oxygen-evolving complex (OEC) of Photosystem II (PSII), is an oxomanganese complex that catalyzes water-splitting into O_2, protons and electrons. Recent breakthroughs in X-ray crystallography have resolved the cuboidal OEC structure at 1.9 Å resolution, stimulating significant interest in studies of structure/function relations. This article summarizes recent advances on studies of the OEC along with studies of synthetic oxomanganese complexes for artificial photosynthesis. Quantum mechanics/molecular mechanics hybrid methods have enabled modeling the S_1 state of the OEC, including the ligation proposed by the most recent X-ray data where D170 is bridging Ca and the Mn center outside the $CaMn_3$ core. Molecular dynamics and Monte Carlo simulations have explored the structural/functional roles of chloride, suggesting that it regulates the electrostatic interactions between D61 and K317 that might be critical for proton abstraction. Furthermore, structural studies of synthetic oxomanganese complexes, including the $[H_2O(terpy)Mn^{III}(\mu\text{-}O)_2Mn^{IV}(terpy)OH_2]^{3+}$ (**1**, terpy=2,2′:6′,2″-terpyridine) complex, provided valuable insights on the mechanistic influence of carboxylate moieties in close contact with the Mn catalyst during oxygen evolution. Covalent attachment of **1** to TiO_2 has been achieved via direct deposition and by using organic chromophoric linkers. The (III,IV) oxidation state of **1** attached to TiO_2 can be advanced to (IV,IV) by visible-light photoexcitation, leading to photoinduced interfacial electron transfer. These studies are particularly relevant to the development of artificial photosynthetic devices based on inexpensive materials.

Introduction

Significant advances in X-ray crystallography of Photosystem II (PSII) were made over the past decade, starting with the first X-ray crystal model of the PSII protein complex obtained at 3.8 Å resolution [1,2]. Subsequent work resolved the structure of PSII at 3.5 Å resolution and proposed a detailed atomistic model of the oxygen-evolving complex (OEC), responsible for catalytic water oxidation [3]. The model included a cuboidal core $CaMn_3$ with a “dangling” Mn, as suggested by EPR studies [4], where the metal centers are linked by μ-oxo bridges (i.e., deprotonated water molecules). However, the positions of the metal centers could not be resolved at 3.5 Å resolution. Nevertheless, the proposed model stimulated significant interest for theoretical studies that built chemically sensible models with a complete coordination of high-valent Mn centers [5–20]. Studies based on density functional theory (DFT), including quantum mechanics/molecular mechanics (QM/MM) structural models with an explicit treatment of the biomolecular environment surrounding the OEC, addressed the nature of the OEC intermediate states along the catalytic cycle as

proposed by Joliot and Kok [21,22]. The models were consistent with available mechanistic data, extended X-ray absorption fine structure (EXAFS) measurements, and Fourier-transform infrared (FTIR) spectroscopy [6–11], although several possible ligation schemes for the nearby amino-acid side chains were found to be possible. These computational models revealed important features of the OEC that have been subsequently confirmed by the most recent X-ray diffraction (XRD) data, including coordination of terminal water molecules bound to the Ca atom and to the dangling Mn, and an additional μ-oxo bridge linking the dangling Mn to the cuboidal $CaMn_3$ cluster (Figure 1) [6–11]. A subsequent X-ray structure, obtained at 3.0 Å resolution, proposed a proteinaceous ligation scheme with bidentate carboxylate groups bridging the metal centers of the OEC [23], although the precise positions of the metal centers, μ-oxo bridges, bound water molecules, side chain ligands, and chloride cofactor still remained unresolved due to radiation damage during the process of X-ray data collection and structural disorder [24–26].

Recent advances in X-ray crystallography have reduced the problem of radiation damage by growing larger crystals and displacing the sample during data collection, and have reported an XRD model of PSII at 1.9 Å resolution [27**]. The model confirmed many structural features common to previous models, including the cuboidal structure of the OEC, the additional μ-oxo bridge linking the dangling Mn to the cuboidal $CaMn_3$ cluster, the presence of terminal water molecules bound to Ca and the dangling Mn, the coordination of nearby amino-acid residues (with carboxylate groups bridging the metal centers), and the presence of chloride in close proximity to the OEC (Figure 1). At the same time, the model introduced features that were not included in any previous empirical or computational models, including the coordination of the side chain of D170 bridging Ca and the dangling Mn. These breakthroughs have stimulated a new series of studies aimed to establish the structure of the OEC and the reaction mechanism, including a DFT QM/MM structural model of the OEC in the dark-adapted (S_1) state consistent with the ligation scheme suggested by the most recent X-ray structure as well as with EXAFS data [28**]. Molecular Dynamics (MD) and Monte Carlo (MC) simulations based on the newest XRD data, have been applied to explore the functional role of chloride as an allosteric regulator of PSII [29**]. In addition, recent DFT QM/MM calculations [30] have been performed to characterize the H-bonding interactions between the carboxylate group of D1-Glu189 bound to Mn(1) and Ca, and the interactions between the redox-active tyrosine Y_Z and the amino-acid residue D1-His190 in close proximity to the OEC.

Mechanistic investigations of the water-splitting reaction also befited from studies of biomimetic oxomanganese complexes [31*,32,33,34*,35,36]. Homogeneous Mn-based systems are catalysts that can be deposited onto semiconductor materials to drive water oxidation in artificial photosynthetic devices [37*,38*]. Many of the mechanistic aspects responsible for water-splitting catalyzed by these oxomanganese synthetic complexes are thought to be common to the OEC of PSII, where a terminal water molecule directly bound to Mn forms an oxyl radical by deprotonation and partial oxidation. The resulting oxyl radical is susceptible to nucleophilic attack by substrate water in close contact with a proton acceptor. Therefore, we address not only recent progress on DFT-QM/MM models of the OEC, including the structural/functional role of cofactors that influence the underlying proton-coupled electron-transfer (PCET) mechanism, but also the characterization of oxomanganese catalysts deposited on nanoparticulate TiO_2 electrode surfaces.

The dark-stable S_1 state of the OEC

In photosynthetic water splitting, the solar energy is used to oxidize the chlorophyll *a* P680, forming the radical $P680^{+\bullet}$, the most oxidizing species known in biology. $P680^{+\bullet}$ is able to oxidize tyrosine Y_Z, which in turn oxidizes the OEC, storing an oxidizing equivalent in the

OEC cluster. The process is repeated, while evolving the OEC through a cycle of S (storage) states [21,22], accumulating 4 oxidizing equivalents before oxygen evolution. The catalytic cycle thus involves five storage states, with S_0 and S_4 the most reduced and oxidized intermediates, respectively. Structural changes in the OEC along the S_0–S_3 transitions have been characterized by X-ray absorption spectroscopy [25,39,40]. Direct comparisons between experimental EXAFS data and simulated spectra based on the most recent XRD structure [25,40] indicate that the XRD model does not correspond to any of the S-state intermediates observed in the catalytic cycle [28**]. Moreover, the comparison to weighted averages of the experimental S_0–S_3 spectra indicate that there is no mixture of S_0–S_3-state intermediates that could give quantitative agreement with the spectrum of the XRD model. Therefore, these theoretical studies concluded that the XRD model corresponds to a mixture of states, more reduced than the S_0 state [28**].

Having ruled out the XRD model as the structure of the S_1 resting state, theoretical work was then focused on obtaining a model of the resting state that is consistent with both the ligation scheme suggested by the new XRD model and with high-resolution EXAFS data. This has been successfully accomplished by the DFT QM/MM model of the OEC in the S_1 Mn_4(IV,III,IV,III) state [28**], shown in Figure 2. In contrast to the X-ray crystal structure, the DFT-QM/MM model is fully consistent with EXAFS data, including polarized EXAFS spectra [41]. Figure 2 shows the structural differences between the XRD and the DFT-QM/MM models and the good agreement between the isotropic and polarized EXAFS spectra of the S_1 state and the corresponding simulated spectra obtained with the DFT-QM/MM model. Quantitative agreement has been obtained [28**] through refinement of the S_1 DFT-QM/MM model (R-QM/MM model in Figure 2) using a conjugate gradient optimization method [10]. These results indicated that disagreement between the EXAFS spectra calculated from the XRD model and the experimental EXAFS spectrum of the S_1 state is primarily due to the absence of Mn-Mn distances shorter than 2.8 Å in the X-ray structure (in chain A).

Chloride cofactor

It has been known for quite some time that chloride depletion from PSII suppresses O_2 evolution by hindering the oxidation of the OEC beyond the S_2 state [42]. However, until very recently, the chloride binding sites and the specific functional/structural roles of chloride have remained elusive [27**,29**,43,44]. Crystallographic studies of bromide- and iodide-substituted PSII samples revealed two binding sites for halide anions in the proximity of the OEC [43], with the most recent XRD data at 1.9 Å resolution confirming the bromide sites (BS1 and BS2) for chloride binding (Figure 1) [27**]. Binding at the BS1 site is stabilized by backbone interactions while binding at the BS2 site involves interactions with the positively charged amino-acid residue D2-Lys317 as well as interactions with water separating D2-Lys317 and D1-Asp61. Those interactions are particularly interesting since amino-acid residues D2-Lys317 and D1-Asp61 belong to a network of polar amino-acid residues suggested to form one of the proton exit channels from the OEC to the lumen [3].

MD and MC simulations based on the DFT-QM/MM model have been applied to explore the effect of chloride binding on specific hydrogen-bonding interactions and protonation states of amino-acid residues at the BS2 binding site [29**]. As shown in Figure 3, the D1-Asp61 side chain occupies a critical position at the BS2 site, between the Mn cluster and the (D2-Lys317)-NH_3^+/Cl^- ion-pair, and is displaced upon Cl^- depletion. These simulations predict that Cl^- depletion alters the hydrogen-bonding interactions of D1-Asp61, inducing the formation of a salt-bridge between the charged side chains of D1-Asp61 and D2-Lys317 (Figure 3). Formation of a stable (and catalytically inactive) salt bridge effectively reduces the D1-Asp61 functionality as a proton acceptor. Therefore, the primary role of Cl^-

suggested by MD and MC simulations is to function as an allosteric regulator of PSII, stabilizing a configuration of charged side chains close to the OEC that favors flexible conformations of the basic center (D1-Asp61), assisting the proton-abstraction at the different S states along the Kok cycle.

Lewis base redox cofactors

DFT QM studies have addressed the redox leveling mechanism based on proton-coupled electron-transfer (PCET) during activation of synthetic oxomanganese catalysts of water oxidation [35,36], including the homogeneous catalyst $[H_2O(terpy)Mn^{III}(\mu\text{-}O)_2Mn^{IV}(terpy)OH_2]^{3+}$ (**1**, terpy=2,2′:6′,2″-terpyridine) [31*,33,34*,45]. These studies also suggested that the reduction potential of **1** is lowered by as much as 100–200 mV upon binding of carboxylate groups (e.g., acetate) that exchange with terminal water ligands. In particular, the analysis of ligand binding free energies and redox potentials indicated that the III,IV → IV,IV oxidation of **1** is facilitated in the presence of acetate (AcO^-) ligands [34]. Analogous to the activation of the OEC, where the oxidized form of Y_Z acts as a primary oxidant and advances the oxidation state of the inorganic core, complex **1** is activated by primary oxidants (e.g., oxone) that generate the high-valent Mn(IV)-$O^{\cdot}$ oxyl intermediate species [45]. This oxyl radical is subject to nucleophilic attack by a substrate water [46], evolving molecular oxygen through formation of a O-O bond, in analogy to photosynthetic O_2 evolution in PSII. Recent DFT studies provided insights on the role of carboxylate moieties in the mechanism of O-O bond formation [Rivalta et al., unpublished data] suggesting that buffer acetate moieties participate as proton acceptors activating the nucleophile water molecules during O-O bond formation and, therefore, reducing the effective potential free energy barrier.

These results are particularly relevant to catalytic water oxidation in PSII, where the OEC cluster is ligated and surrounded by carboxylate groups of polar amino-acid side chains, including Asp170, Glu189, Glu333, Glu354, Ala344, Asp342 and Asp61 (Figure 1). In particular, D1-Asp61 is directly interacting with the OEC through various H-bond interactions and could function as a proton acceptor in the presence of chloride. D1-Glu189 is the only amino-acid residue with a carboxylate group that binds the OEC as a monodentate ligand. The carboxylate oxygen not bound to the Mn center is H-bonded to a water molecule W_1^* bound to Ca, suggesting that it could also be responsible for proton abstraction from W_1^*, during a nucleophilic attack of W_1^* onto the oxyl radical Mn(IV)-$O^{\cdot}$ formed upon deprotonation and partial oxidation of the water ligand W_2^*. Another interesting feature is that D1-Asp170 is bridging between the Ca and the dangling Mn, the two metal centers with terminal water ligands. Therefore, there is the nontrivial question as to whether D1-Asp170 might remain in that binding mode or otherwise assume other configurations that would allow this carboxylate group to participate in the deprotonation of substrate water molecules.

Biomimetic Mn catalysts for artificial photosynthesis

Solar cells that efficiently convert water into H_2 and O_2 require coupling of water-oxidation catalysts to electrode surfaces. Inexpensive homogeneous catalysts are ideal candidates for heterogeneous assemblies based on surface covalent attachment. In particular, assemblies of Mn biomimetic complexes to semiconductor electrodes, such as TiO_2 thin-films, are particularly attractive for large-scale applications of photocatalytic solar cells [47*].

Recent work has focused on studies of TiO_2 nanoparticles (NPs) functionalized with complex **1** via direct adsorption [37*], or by attachment through light-harvesting organic linkers that are robust under aqueous and oxidative conditions [38*]. Figure 4 shows a

molecular model of a functionalized TiO_2 NP using complex **1**, where the mixed-valence (III,IV) state of **1** attaches to near-amorphous TiO_2 NPs by substituting one of its water ligands by the TiO_2 NP, as suggested by low-temperature (7 K) EPR data and DFT QM/MM modeling. Characterization of **1**–TiO_2 hybrid assemblies using three TiO_2 materials with different degrees of crystallinity (P25, with 85% anatase, D450, with NP sintered at 450 °C and mainly constituted by anatase, and D70, with low crystallinity) indicates that the (III,IV) Mn dimer is not the predominant form of the surface adsorbate complex for well-crystallized TiO_2 nanoparticles, probably due to formation of Mn(IV) tetramers. Using Ce^{4+} as a primary oxidant, oxygen evolution was observed for **1**–P25, as shown in Figure 4. When covalently attached via chromophoric organic linkers, the Mn(III,IV) state could be advanced to the Mn(IV,IV) state by visible-light photoexcitation leading to photoinduced interfacial electron transfer [38*]. These results are particularly relevant to the development of photocatalytic devices for oxidation chemistry based on inexpensive materials (e.g., TiO_2 and Mn complexes).

Conclusions

Recent advances in studies of natural and artificial photosynthesis have provided valuable insights on the nature of the catalytic centers responsible for water-oxidation in PSII and biomimetic catalysts based on inexpensive, earth-abundant materials. Computational studies have addressed fundamental questions, stimulated by recent breakthroughs in X-ray crystallography, including the structure of the OEC of PSII and the potential functional roles of acid/base and redox cofactors that are essential for photosynthetic water oxidation. Work in progress involves the characterization of the intermediate S states, taking into account the potential functional roles of essential cofactors such as chloride ions and Lewis base carboxylate groups that might be essential for the activation mechanism based on PCET. The resulting insight is particularly valuable for the development of synthetic catalytic systems with common mechanistic functionalities, where photoabsorption, PCET and IET are essential for activation of the catalyst. These studies are, thus, expected to make many more important contributions to the development of photocatalytic solar cells through the integrated effort of computational modeling and high-resolution spectroscopic techniques, in conjunction with ligand design, synthesis and assembly to electrode surfaces.

Acknowledgments

V.S.B. acknowledges financial support from the Division of Chemical Sciences, Geosciences, and Biosciences, Office of Basic Energy Sciences, U.S. Department of Energy (DE-SC000-1423), and supercomputer time from National Energy Research Scientific Computing. NIH grants GM84267 and GM043278 supported the development of methods implemented in the studies. Studies of oxomanganese complexes for artificial photosynthesis were supported by the Office of Basic Energy Sciences of the U.S. Department of Energy (DE-FG02-07ER15909). G.W.B. acknowledges support from NIH Grant GM32715 and U.S. Department of Energy grant DE-FG02-05ERI5646 for work on PSII.

References and recommended reading

Papers of particular interest, published within the period of review, have been highlighted as:

(*) of special interest

(**) of outstanding interest

1. Rhee KH. Photosystem II: The solid structural era. Annu Rev Biophys Biomol Struct. 2001; 30:307–328. [PubMed: 11340062]

2. Zouni A, Witt HT, Kern J, Fromme P, Krauss N, Saenger W, Orth P. Crystal structure of photosystem II from Synechococcus elongatus at 3. 8 angstrom resolution. Nature. 2001; 409:739–743. [PubMed: 11217865]
3. Ferreira KN, Iverson TM, Maghlaoui K, Barber J, Iwata S. Architecture of the photosynthetic oxygen-evolving center. Science. 2004; 303:1831–1838. [PubMed: 14764885]
4. Britt R, Campbell K, Peloquin J, Gilchrist M, Aznar C, Dicus M, Robblee J, Messinger J. Recent pulsed EPR studies of the photosystem II oxygen-evolving complex: implications as to water oxidation mechanisms. BBA-Bioenergetics. 2004; 1655:158–171. [PubMed: 15100028]
5. Cox N, Rapatskiy L, Su JH, Pantazis DA, Sugiura M, Kulik L, Dorlet P, Rutherford AW, Neese F, Boussac A, et al. Effect of Ca^{2+}/Sr^{2+} Substitution on the Electronic Structure of the Oxygen-Evolving Complex of Photosystem II: A Combined Multifrequency EPR, (55)Mn-ENDOR, and DFT Study of the S_2 State. J Am Chem Soc. 2011; 133:14149–14149.
6. Sproviero EM, Gascon JA, McEvoy JP, Brudvig GW, Batista VS. QM/MM models of the O_2-evolving complex of photosystem II. J Chem Theory Comput. 2006; 2:1119–1134.
7. Sproviero EM, Gascon JA, McEvoy JP, Brudvig GW, Batista VS. Quantum mechanics/molecular mechanics structural models of the oxygen-evolving complex of photosystem II. Curr Opin Struct Biol. 2007; 17:173–180. [PubMed: 17395452]
8. Sproviero EM, Gascon JA, McEvoy JP, Brudvig GW, Batista VS. Quantum mechanics/molecular mechanics study of the catalytic cycle of water splitting in photosystem II. J Am Chem Soc. 2008; 2:3428–3442. [PubMed: 18290643]
9. Sproviero EM, Gascon JA, McEvoy JP, Brudvig GW, Batista VS. Computational studies of the O_2-evolving complex of photosystem II and biomimetic oxomanganese complexes. Coord Chem Rev. 2008; 252:395–415. [PubMed: 19190716]
10. Sproviero EM, Gascon JA, McEvoy JP, Brudvig GW, Batista VS. A Model of the Oxygen-Evolving Center of Photosystem II Predicted by Structural Refinement Based on EXAFS Simulations. J Am Chem Soc. 2008; 130:6728–6730. [PubMed: 18457397]
11. Sproviero EM, Shinopoulos K, Gascon JA, McEvoy JP, Brudvig GW, Batista VS. QM/MM computational studies of substrate water binding to the oxygen-evolving centre of photosystem II. Philos T R Soc B. 2008; 363:1149–1156.
12. Lundberg M, Siegbahn PEM. Theoretical investigations of structure and mechanism of the oxygen-evolving complex in PSII. Phys Chem Chem Phys. 2004; 6:4772–4780.
13. Siegbahn PEM, Lundberg M. The mechanism for dioxygen formation in PSII studied by quantum chemical methods. Photoch Photobio Sci. 2005; 4:1035–1043.
14. Siegbahn PEM. O-O bond formation in the S_4 state of the oxygen-evolving complex in photosystem II. Chem Eur J. 2006; 12:9217–9227. [PubMed: 17029313]
15. Siegbahn EM. A Structure-Consistent Mechanism for Dioxygen Formation in Photosystem II. Chem Eur J. 2008; 14:8290–8302. [PubMed: 18680116]
16. Siegbahn PEM. Mechanism and energy diagram for O-O bond formation in the oxygen-evolving complex in photosystem II. Philos T R Soc B. 2008; 363:1221–1228.
17. Siegbahn PEM. Theoretical studies of O-O bond formation in photosystem II. Inorg Chem. 2008; 47:1779–1786. [PubMed: 18330969]
18. Siegbahn PEM. An Energetic Comparison of Different Models for the Oxygen Evolving Complex of Photosystem II. J Am Chem Soc. 2009; 131:18238. [PubMed: 19961231]
19. Siegbahn PEM. Structures and Energetics for O_2 Formation in Photosystem II. Acc Chem Res. 2009; 42:1871–1880. [PubMed: 19856959]
20. Schinzel S, Schraut J, Arbuznikov AV, Siegbahn PEM, Kaupp M. Density Functional Calculations of (55)Mn, (14)N and (13)C Electron Paramagnetic Resonance Parameters Support an Energetically Feasible Model System for the S_2 State of the Oxygen-Evolving Complex of Photosystem II. Chem Eur J. 2010; 16:10424–10438. [PubMed: 20645339]
21. Joliot P, Barbieri G, Chabaud R. A New Model of Photochemical Centers in System-2. Photochem Photobiol. 1969; 10:309.
22. Kok B, Forbush B, McGloin M. Cooperation of Charges in Photosynthetic O_2 Evolution.1. A Linear 4step Mechanism. Photochem Photobiol. 1970; 11:457. [PubMed: 5456273]

23. Loll B, Kern J, Saenger W, Zouni A, Biesiadka J. Towards complete cofactor arrangement in the 3. 0 angstrom resolution structure of photosystem II. Nature. 2005; 438:1040–1044. [PubMed: 16355230]

24. Yano J, Kern J, Irrgang K, Latimer M, Bergmann U, Glatzel P, Pushkar Y, Biesiadka J, Loll B, Sauer K, et al. X-ray damage to the Mn4Ca complex in single crystals of photosystem II: A case study for metalloprotein crystallography. Proc Natl Acad Sci USA. 2005; 102:12047–12052. [PubMed: 16103362]

25. Dau H, Liebisch P, Haumann M. The structure of the manganese complex of Photosystem II in its dark-stable S_1-state: EXAFS results in relation to recent crystallographic data. Phys Chem Chem Phys. 2004; 6:4781–4792.

26. Grabolle M, Haumann M, Muller C, Liebisch P, Dau H. Rapid loss of structural motifs in the manganese complex of oxygenic photosynthesis by x-ray irradiation at 10–300 K. J Biol Chem. 2006; 281:4580–4588. [PubMed: 16352605]

27**. Umena Y, Kawakami K, Shen J-R, Kamiya N. Crystal structure of oxygen-evolving photosystem II at a resolution of 1. 9 Å. Nature. 2011; 473:55–60. X-ray diffraction model of PSII from the cyanobacterium Thermosynechococcus vulcanus at 1.9 Å resolution. The position and coordination of metal centers in the oxygen-evolving complex (OEC) were resolved from the electron density map, showing a cubane-like Mn_3CaO_4 cluster linked to a fourth Mn, with an addition μ-oxo bridge. Most of carboxylate groups bridge the metal centers, including the side chain of D170 bridging Ca and the dangling Mn, a features that was not included in any previous OEC model. Four water molecules were bound to the Mn cluster, including a water bound to Ca and another one bound to the Mn outside the cube. In addition, two chloride ions were located in close proximity to the OEC. [PubMed: 21499260]

28**. Luber S, Rivalta I, Umena Y, Kawakami K, Shen J-R, Kamiya N, Brudvig GW, Batista VS. S_1-State Model of the O_2-Evolving Complex of Photosystem II. Biochemstry. 2011; 50:6308–6311. Quantum Mechanics/Molecular Mechanics (QM/MM) model of the OEC of PSII in the dar-stable S1 Mn_4(IV, III, IV, III) state, where Ca^{2+} is bridged to manganese centers by the carboxylate moieties of D170 and A344, consistently with the most recent X-ray diffraction model reported at 1.9 Å resolution. The model is also consistent with high-resolution spectroscopic data, including isotropic and polarized extended X-ray absorption fine structure data. Refined intermetallic distances within the Mn cluster were provided, suggesting that the XRD model most likely corresponds to a mixture of reduced states.

29**. Rivalta I, Amin M, Luber S, Vassiliev S, Pokhrel R, Umena Y, Kawakami K, Shen J-R, Kamiya N, Bruce D, et al. Structural-Functional Role of Chloride in Photosystem II. Biochemistry. 2011; 50:6312–6315. Analysis of the potential functional role of chloride ions in PSII, based on the binding sites revealed in the X-ray crystal structure of PSII at 1.9 Å resolution. It is shown, that chloride depletion induces formation of a salt bridge between D2 and D1 subunits, involving charged side chains of D2-K317 and D1-D61 amino acid residues. The formation of a stable (and catalytically inactive) salt bridge would effectively reduce the D1-Asp61 functionality as a proton acceptor and this could suppress the transfer of protons from the OEC to the lumen. [PubMed: 21678923]

30. Saito K, Shen J-R, Ishida T, Ishikita H. Short Hydrogen Bond between Redox-Active Tyrosine Y_Z and D1-His190 in the Photosystem II Crystal Structure. Biochemistry. 2011; 50:9836–9844. [PubMed: 21972783]

31*. Cady CW, Shinopoulos KE, Crabtree RH, Brudvig GW. (H_2O)(terpy)Mn(μ-O)$_2$Mn(terpy)$(OH_2)(NO_3)_3$ (terpy=2,2′:6,2″-terpyridine) and its relevance to the oxygen-evolving complex of photosystem II examined through pH dependent cyclic voltammetry. Dalton T. 2010; 39:3985–3989. In this paper, the electrochemical behavior of the biomimetic water-oxidation catalyst $[H_2O(terpy)Mn^{III}(\mu\text{-}O)_2Mn^{IV}(terpy)OH_2]^{3+}$ (**1**, terpy=2,2′:6′,2″-terpyridine) has been examined in water under a variety of pH and buffered conditions. In the presence of an acetate buffer, a carboxylate group binds to **1** in place of one of the terminal water ligands. Experimental evidences show that **1** exhibits proton-coupled electron-transfer reactivity analogous to the OEC, and may be capable of electrochemical water oxidation.

32. Tagore R, Chen HY, Crabtree RH, Brudvig GW. Determination of mu-oxo exchange rates in di-mu-oxo dimanganese complexes by electrospray ionization mass spectrometry. J Am Chem Soc. 2006; 128:9457–9465. [PubMed: 16848483]

33. Wang T, Brudvig G, Batista VS. Characterization of Proton Coupled Electron Transfer in a Biomimetic Oxomanganese Complex: Evaluation of the DFT B3LYP Level of Theory. J Chem Theory Comput. 2010; 6:755–760. [PubMed: 20607115]

34*. Wang T, Brudvig GW, Batista VS. Study of Proton Coupled Electron Transfer in a Biomimetic Dimanganese Water Oxidation Catalyst with Terminal Water Ligands. J Chem Theory Comput. 2010; 6:2395–2401. In this work, the (III,IV) → (IV,IV) one-electron oxidation of the catalyst $[H_2O(terpy)Mn^{III}(\mu\text{-}O)_2Mn^{IV}(terpy)OH_2]^{3+}$ (**1**, terpy=2,2′:6′,2″-terpyridine) has been studied and compared to the analogous conversion in an oxomanganese complex without terminal water ligands, the $[(bpy)_2\ Mn^{III}(\mu\text{-}O)_2\ Mn^{IV}(bpy)_2]^{3+}$ complex (**2**, bpy=2,2′-bipyridyl). The oxidative transition has been analyzed in terms of free energy calculations of redox potentials and pKa's as directly compared to cyclic voltammogram measurements. The pKa's of terminal water ligands depend strongly on the oxidation states of the metal centers, and the oxidation potential of **1** is strongly dependent on pH (in contrast to **2**) as well as by coordination of Lewis base moieties (e.g., carboxylate groups) that competitively bind to Mn by exchange with terminal water ligands. [PubMed: 20827389]

35. Luo S, Rivalta I, Batista V, Truhlar DG. Noncollinear Spins Provide a Self-Consistent Treatment of the Low-Spin State of a Biomimetic Oxomanganese Synthetic Trimer Inspired by the Oxygen Evolving Complex of Photosystem II. J Phys Chem Lett. 2011; 2:2629–2633.

36. Cady CW, Crabtree RH, Brudvig GW. Functional models for the oxygen-evolving complex of photosystem II. Coord Chem Rev. 2008; 252:444–455. [PubMed: 21037800]

37*. Li G, Sproviero EM, Snoeberger RC III, Iguchi N, Blakemore JD, Crabtree RH, Brudvig GW, Batista VS. Deposition of an oxomanganese water oxidation catalyst on TiO_2 nanoparticles: computational modeling, assembly and characterization. Energ Environ Sci. 2009; 2:230–238. In this paper, a successful attachment of the catalyst $[H_2O(terpy)Mn^{III}(\mu\text{-}O)_2Mn^{IV}(terpy)OH_2]^{3+}$ (**1**, terpy=2,2′:6′,2″-terpyridine) has been onto TiO_2 nanoparticles (NPs) via direct adsorption, or in situ synthesis, has been reported. The **1**-TiO_2 surface complexes have been characterized with a variety of techniques, including EPR and UV-visible spectroscopy, electrochemical measurements and computational modeling. The mixed-valence (III,IV) state of 1 attaches to near-amorphous TiO_2 NPs by substituting one of its water ligands by the TiO_2 NP. Using Ce^{4+} as a primary oxidant, oxygen evolution was observed for assemblies of complex **1** attached to highly crystalline NP.

38*. Li G, Sproviero EM, McNamara WR, Snoeberger RC III, Crabtree RH, Brudvig GW, Batista VS. Reversible Visible-Light Photooxidation of an Oxomanganese Water-Oxidation Catalyst Covalently Anchored to TiO_2 Nanoparticles. J Phys Chem B. 2010; 114:14214–14222. This paper reports the covalent attachment of of the catalyst $[H_2O(terpy)Mn^{III}(\mu\text{-}O)_2Mn^{IV}(terpy)OH_2]^{3+}$ (**1**, terpy=2,2′:6′,2″-terpyridine) has been onto nanoparticulate TiO_2 surfaces (NP) using a robust chromophoric linker. The organic linker (**L**) is a phenylterpy ligand attached to a 3-phenylacetylacetonate anchoring moiety via an amide bond, and it absorbs visible light, leading to photoinduced interfacial electron transfer into the semiconductor conduction band. The Mn(III,IV) state of **1** can be reversibly advanced to the Mn(IV,IV) state by visible-light photoexcitation of **1**-**L**-TiO_2. A high degree of crystallinity of the TiO2 NPs is essential for promoting photooxidation of the adsorbates by photoinduced charge separation. [PubMed: 19924873]

39. Sauer K, Yano J, Yachandra VK. X-ray spectroscopy of the photosynthetic oxygen-evolving complex. Coord Chem Rev. 2008; 252:318–335. [PubMed: 19190720]

40. Haumann M, Muller C, Liebisch P, Iuzzolino L, Dittmer J, Grabolle M, Neisius T, Meyer-Klaucke W, Dau H. Structural and oxidation state changes of the photosystem II manganese complex in four transitions of the water oxidation cycle (S_0->S_1, S_1->S_2, S_2->S_3, and $S_{3,4}$->S_0) Characterized by X-ray absorption spectroscopy at 20 K and room temperature. Biochemistry. 2005; 44:1894–1908. [PubMed: 15697215]

41. Yano J, Kern J, Sauer K, Latimer MJ, Pushkar Y, Biesiadka J, Loll B, Saenger W, Messinger J, Zouni A, et al. Where water is oxidized to dioxygen: Structure of the photosynthetic Mn_4Ca cluster. Science. 2006; 314:821–825. [PubMed: 17082458]

42. Wincencjusz H, van Gorkom HJ, Yocum CF. The photosynthetic oxygen evolving complex requires chloride for its redox state S_2->S_3 and S_3->S_0 transitions but not for S_0->S_1 or S_1->S_2 transitions. Biochemistry. 1997; 36:3663–3670. [PubMed: 9132019]

43. Murray JW, Maghlaoui K, Kargul J, Ishida N, Lai TL, Rutherford AW, Sugiura M, Boussac A, Barber J. X-ray crystallography identifies two chloride binding sites in the oxygen evolving centre of Photosystem II. Energ Environ Sci. 2008; 1:161–166.

44. Guskov A, Kern J, Gabdulkhakov A, Broser M, Zouni A, Saenger W. Cyanobacterial photosystem II at 2. 9-angstrom resolution and the role of quinones, lipids, channels and chloride. Nat Struct Mol Biol. 2009; 16:334–342. [PubMed: 19219048]

45. Limburg J, Vrettos JS, Chen HY, de Paula JC, Crabtree RH, Brudvig GW. Characterization of the O_2-evolving reaction catalyzed by $(H_2O)(terpy)Mn(\mu\text{-}O)_2Mn(terpy)(OH_2)(NO_3)_3$ (terpy=2,2′:6,2″-terpyridine). J Am Chem Soc. 2001; 123:423–430. [PubMed: 11456544]

46. Lundberg M, Blomberg MRA, Siegbahn PEM. Oxyl radical required for O-O bond formation in synthetic Mn-catalyst. Inorg Chem. 2004; 43:264–274. [PubMed: 14704076]

47*. Batista, VS. Some Computational Challenges in Energy Research. In: Crabtree, RH., editor. Energy Production and Storage – Inorganic Chemical Aspects. Wiley; 2010. p. 191-198.This article reviews recent advances in the fundamental understanding of structure/function relationships in inexpensive photocatalytic materials for fuel production, with emphasis on computational work for the development and characterization of catalytic surfaces based on nanoporous TiO_2 thin films functionalized with Mn catalysts. The reviewed compuitational studies have been integrated with synthesis, spectroscopy, and electrochemistry experimental work

Highlights

- The dark-stable S_1 state of the oxygen evolving complex (OEC) of Photosystem II has been recently modeled using quantum mechanics/molecular mechanics (QM/MM) hybrid methods that explicitly describe the surrounding biomolecular environment consistently with the X–ray structure resolved at 1.9 Å resolution
- Molecular Dynamics and Monte Carlo studies based on the DFT-QM/MM model of the OEC have shown that chloride regulates the formation of a salt-bridge of polar amino acids next OEC that are thought to be involved in proton abstraction
- DFT studies have shown that carboxylate groups can function as redox and acid/base cofactors during oxidation state transitions of oxomanganese complexes
- DFT QM/MM modeling and experimental studies of Mn catalysts covalently bound to TiO_2 semiconductors, have characterized the surface attachment mode and confirmed oxygen evolution driven by a one-electron primary oxidant.

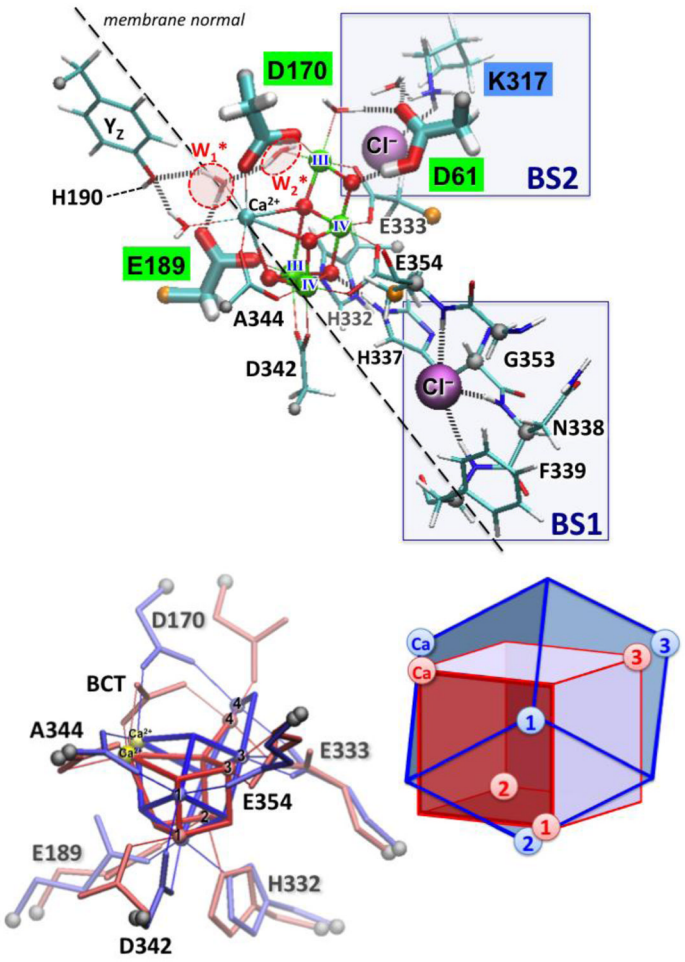

Fig 1.

The oxygen-evolving complex (OEC) of Photosystem II (PSII). Top panel: ligation scheme of the Mn_4O_5Ca cluster and chloride binding sites (BS1 and BS2) as proposed by the X-ray model at 1.9 Å resolution. Carboxylate groups of amino-acid residues in close contact with the OEC, including D1-Asp61, D1-Asp170 and D1-Glu189 that might be essential for proton-transfer events along the catalytic cycle of water oxidation are highlighted. Bottom panel: Superposition of the OEC in the X-ray models of PSII at 1.9 Å (blue) and 3.5 Å (red) resolution. Bottom part reproduced from Ref. 28**.

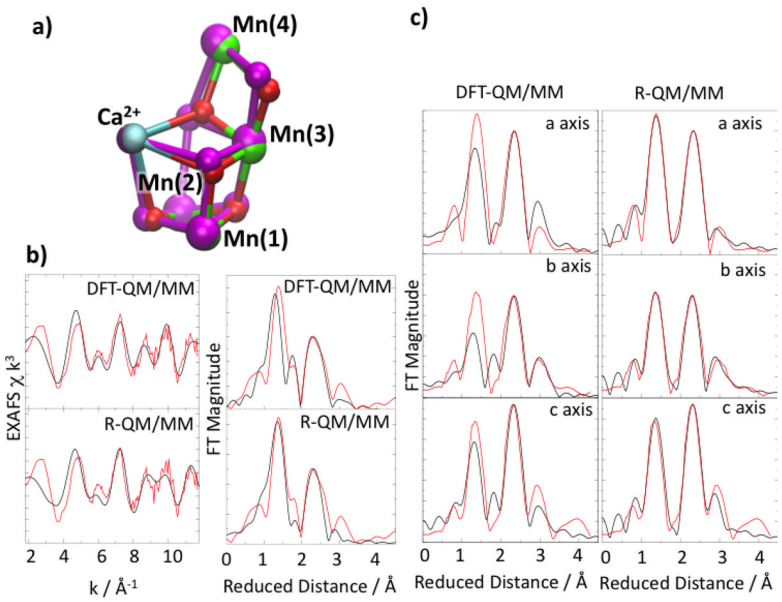

Fig 2.

Superposition of the new XRD model and the DFT-QM/MM S_1 state model of the OEC (panel a). Comparison between experimental (red) and calculated (black) isotropic (panel b) and polarized (panel c) EXAFS spectra for the OEC of PSII in the S_1 state calculated with the DFT-QM/MM and refined R-QM/MM model. Reproduced from Ref. 28**.

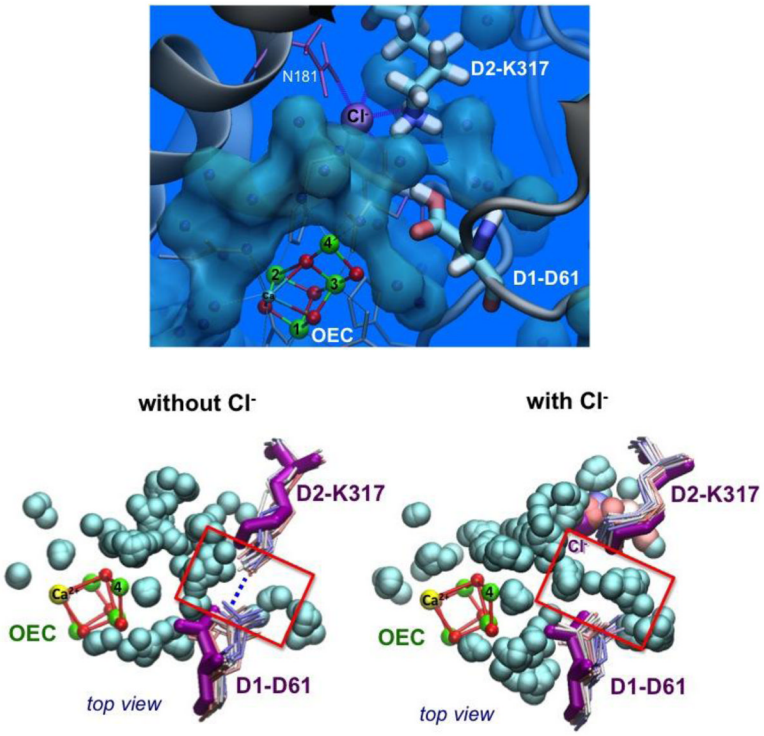

Fig 3.

Top: Waters modeled in the 1.9 Å X-ray structure (gray spheres) next to the Cl^{-}, OEC, and residues D1-Asp61 (D61) and D2-Lys317 (K317). Bottom: Superposition of instantaneous configurations along MD simulations (waters shown as gray spheres and D61, K317 side chains colored from red to blue for 0–24 ns) of the OEC with (right) or without (left) Cl^{-} at the BS2 site. A salt-bridge between K317 and D61 forms upon Cl^{-} depletion, and is interrupted by water in the presence of Cl^{-}. The X-ray configuration is shown in magenta. Reproduced from Ref. 29**.

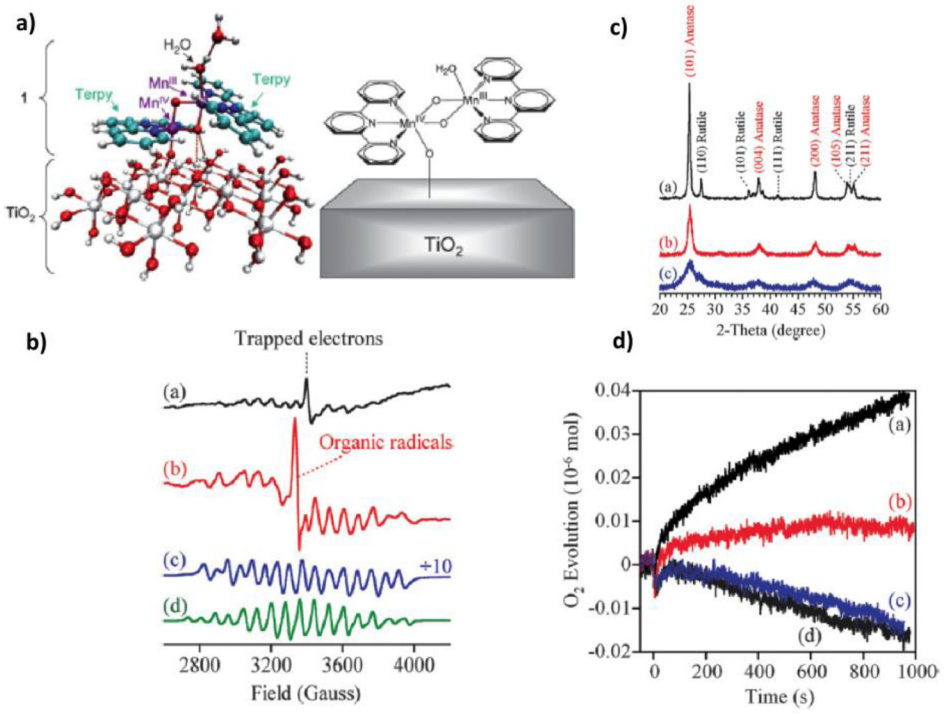

Fig 4.

Panel a: DFT/QM-QMM model of the complex 1 anchored to a TiO_2–NP, with a water ligand exchanged by the NP. Color scheme: C (lightblue), H (white), Mn (purple), N (blue), O (red), Ti (gray). Panel b: EPR spectra of (a) **1**–P25, (b) **1**–D450, (c) **1**–D70, and (d) complex **1** in a HOAc/NaOAc buffer solution (pH 4.5) is also shown in the figure (d). A trapped electron signal and an organic radical signal are present in spectra (a) and (b), respectively. Panel c: Powder XRD patterns of (a) P25, (b) D450, and (c) D70 indicating different crystallinity of these TiO_2 nanoparticles. Panel d: O_2 evolution using Ce^{4+} as a single-electron oxidant. **1** was loaded on TiO_2 (50 mg) samples: (a) P25, (b) D450, and (c) D70; and control test using (d) bare P25 NP's as the catalyst. Reproduced from Ref. 37.